Available online at www.sciencedirect.com
ScienceDirect
Tetrahedron
Tetrahedron 63 (2007) 7985–7996

Adamantane-retropeptides, new building blocks for molecular channels

Nikola Basarić, Krešimir Molčanov, Marija Matković, Biserka Kojić-Prodić* and Kata Mlinarić-Majerski*

Ruđer Bošković Institute, Bijenička cesta 54, PO Box 180, 10 002 Zagreb, Croatia

Received 7 February 2007; revised 27 April 2007; accepted 17 May 2007
Available online 24 May 2007

Abstract—Novel adamantane-oxalamide derivatives, *N*,*N*′-bis(1-adamantylglycine methyl ester)oxalamide (*meso*-**1** and *rac*-**1**), *N*,*N*′-bis(3-aminoadamantane-1-carboxylic acid methyl ester)oxalamide (**2**) and *N*,*N*′-bis(3-aminoadamantane-1-carboxylic acid)oxalamide (**3**) were prepared and structurally characterized by spectroscopic methods and X-ray analysis. Crystal packing of the structures *meso*-**1** and *rac*-**1** is defined by one-dimensional α-networks of hydrogen-bonded chains. The crystal structures of **2** and **3** are characterized by two-dimensional β-networks of hydrogen bonds. The oxalamide **3** crystallizes as the solvates only. In the crystal structure of **3** the protic solvent participates in hydrogen bonding with the oxalamide moieties. However, in non-protic solvents **3** crystallizes as a solvate but the solvent does not participate in hydrogen bonding. The two-dimensional network of hydrogen bonds connecting molecules of **3** generates channels, which are filled by discrete solvent molecules.

1. Introduction

Synthesis of peptidomimetics has attracted considerable attention in recent years, mainly because of their numerous applications, primarily as biologically active molecules.[1] A special interest in the chemistry of peptidomimetics has been directed towards the synthesis of cyclic peptides and depsipeptides containing unnatural amino acids.[2] These compounds have shown extremely good properties in the solid state forming tubular structures or ion channels.[3] Since these structures may find applications in nanotechnology, the synthesis of new derivatives is under intensive investigation. Therefore, in continuation of that research it is important to synthesize new synthons, which could be used later on as building blocks in the coupling reactions and preparation of more complex molecules. Moreover, the structural role of new synthons could be explored in the design of new macrocycles or peptidomimetics with tailor-made structural and functional characteristics.

In the scope of our research on chemistry of polycyclic molecules[4] and their application as versatile building blocks,[5] we turned our attention to the synthesis of unnatural amino acids[6] and hydroxyacids, which incorporate adamantane as a building block.[7] The spacious adamantyl cage is a highly lipophilic group and can affect the bioavailability of peptidomimetics significantly. We showed that incorporation of unnatural amino acids derived from adamantanes in the methionine-enkephalin peptide increased the lipophilicity of the peptide facilitating its transport through the cell membrane. Since methionine-enkephalin derivatives showed good in vitro anticancer properties these molecules are promising candidates for the development of new anticancer agents.[6]

In this paper, we report the synthesis of four new oxalamide retropeptides with adamantane subunits, *meso*-**1**, *rac*-**1**, **2** and **3** (Schemes 1 and 2), and their structural characterization. The oxalamide derivatives have shown a tendency to form two-dimensional hydrogen-bonding β-networks.[8] Moreover, some oxalamide amino acid derivatives showed good properties in forming gels with non-polar and polar solvents.[9] Incorporation of adamantanes as bulky substituents in these compounds is expected to affect conformational mobility and the hydrogen-bonding motifs. Therefore, it is anticipated that these oxalamide-adamantane derivatives would show different structural motifs in the solid state, depending on the substitution on the adamantane skeleton. Additionally, knowledge of the structure of these oxalamides may be useful for docking and prediction of potential biological activity.

Keywords: Adamantane-oxalamides; Molecular channels; Retropeptides; Synthesis; X-ray structural analysis.
* Corresponding authors. Fax: +385 1 46 80 195 (K.M.-M.); fax: +385 1 46 80 245 (B.K.-P.); e-mail addresses: kojic@irb.hr; majerski@irb.hr

0040–4020/$ - see front matter © 2007 Elsevier Ltd. All rights reserved.
doi:10.1016/j.tet.2007.05.066

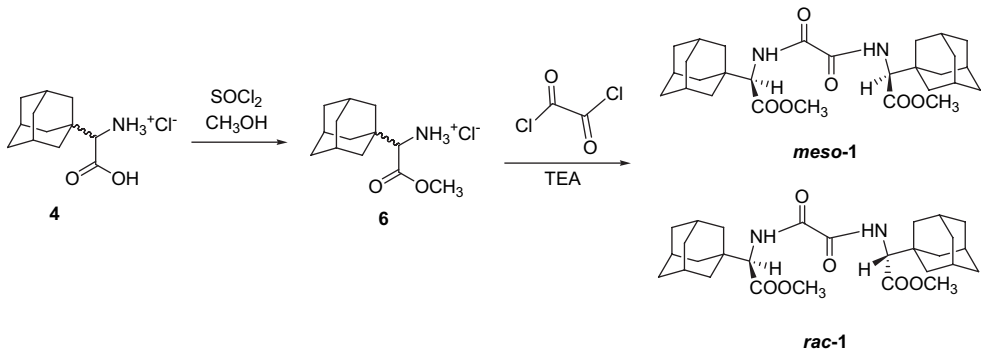

Scheme 1.

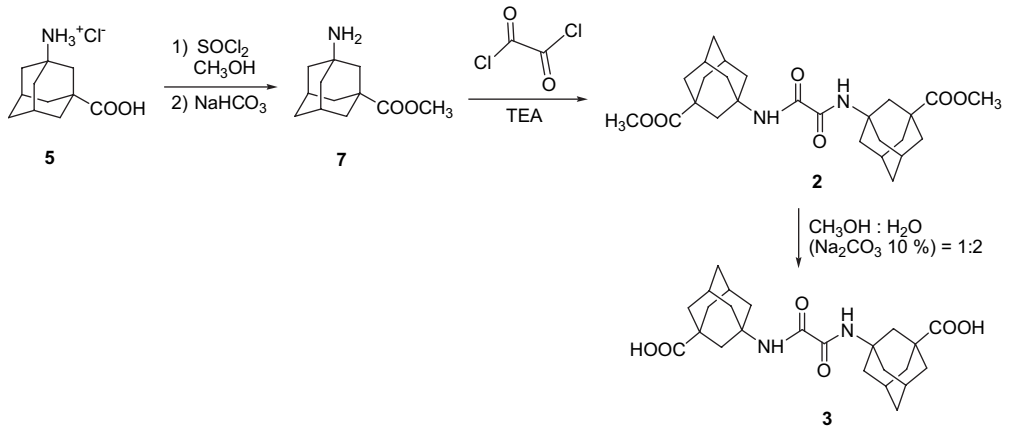

Scheme 2.

2. Results and discussion

2.1. Synthesis

Synthesis of the adamantane amino acids **4** and **5** was performed according to the described procedure,[6,10] and the corresponding hydrochlorides were transformed to their methyl esters **6** and **7**, respectively (Schemes 1 and 2). Due to the steric bulkiness imposed by adamantane moiety, the esterification was difficult, but it was accomplished in a good yield after several days of refluxing in methanol in the presence of $SOCl_2$. Oxalamides **1** and **2** were obtained from esters **6** and **7**, respectively, in a reaction with oxalyl chloride in the presence of triethylamine. The reaction of glycine derivative **6** furnished mixture of two diastereomers *meso*-**1** and *rac*-**1**, which were separated by preparative TLC. The oxalamide derivatives *meso*-**1**, *rac*-**1** and **2** were characterized by spectroscopic methods. In their ^{1}H NMR spectra, a signal at δ ~7 ppm was present, which was assigned to the oxalamide NH protons. In the ^{13}C NMR spectra the corresponding oxalamide C═O signal was present at ~159 ppm, whereas signals at 169 ppm in the ^{13}C NMR spectra of **1** or 176 ppm in the ^{13}C NMR spectra of **2** were assigned to the chemical shifts of the ester C═O. The signals corresponding to the adamantane resonances in the ^{13}C NMR spectra indicated highly symmetric structures characterized by one singlet, one doublet and two triplets in the spectra of *meso*-**1** and *rac*-**1**, or two singlets, one doublet and four triplets in the ^{13}C NMR spectrum of **2**.

In order to obtain building blocks, which could be incorporated into bigger molecules, we transformed retropeptide-esters **1** and **2** to the corresponding diacid derivatives. The hydrolysis turned out to be difficult, probably due to the steric hindrance of bulky adamantane moieties. Thus, upon treatment of retropeptide-esters **2** at rt with a 1 M solution of LiOH or saturated NaOH, only starting material was recovered. However, the ester hydrolysis was accomplished in a mixture of boiling methanol and 10% aqueous Na_2CO_3 (in a ratio of 1:2). In that way, diacid **3** was isolated in good yield, but diacids obtained from the mixture of diastereomers **1** were highly insoluble and we could not proceed with the diastereomer separation and their independent characterization.

The ester derivatives of oxalamides *meso*-**1**, *rac*-**1** and **2**, as well as diacid derivative **3** showed no tendency to form gels with organic solvents or water.

2.2. Crystal structures

The single crystals of the ester derivatives *meso*-**1**, *rac*-**1** and **2** were easily obtained, whereas unexpected problems were encountered in attempts to crystallize compound **3**. Apparently it crystallizes only in the form of relatively unstable solvates. Molecular structures of the compounds *meso*-**1**, *rac*-**1**, **2**, **3**·MeOH and **3**·EtOAc are shown in Figures 1–5. Achiral compounds *meso*-**1**, **2** and **3**·MeOH (Figs. 1, 3 and 4, respectively) have a molecular C_i symmetry (crystallographic

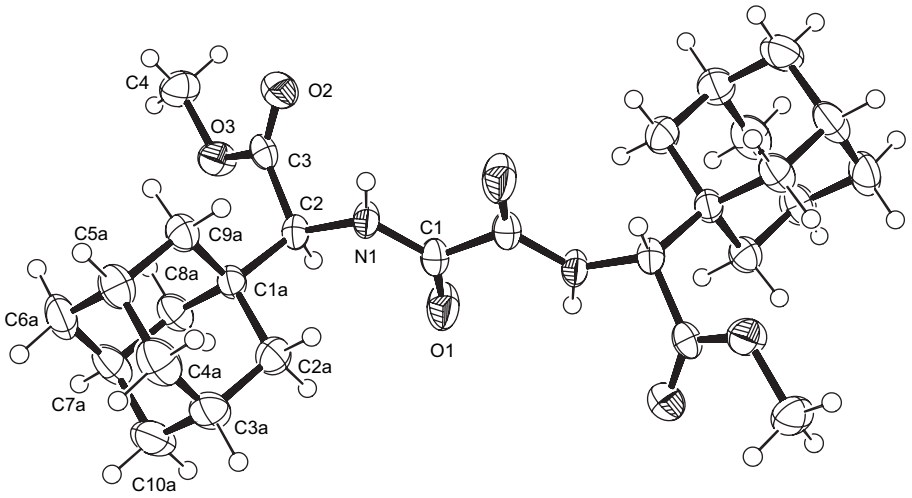

Figure 1. The molecular structure of *meso*-**1** with the atom numbering scheme. Thermal ellipsoids are drawn at the 50% probability level. The molecular symmetry is C_i.

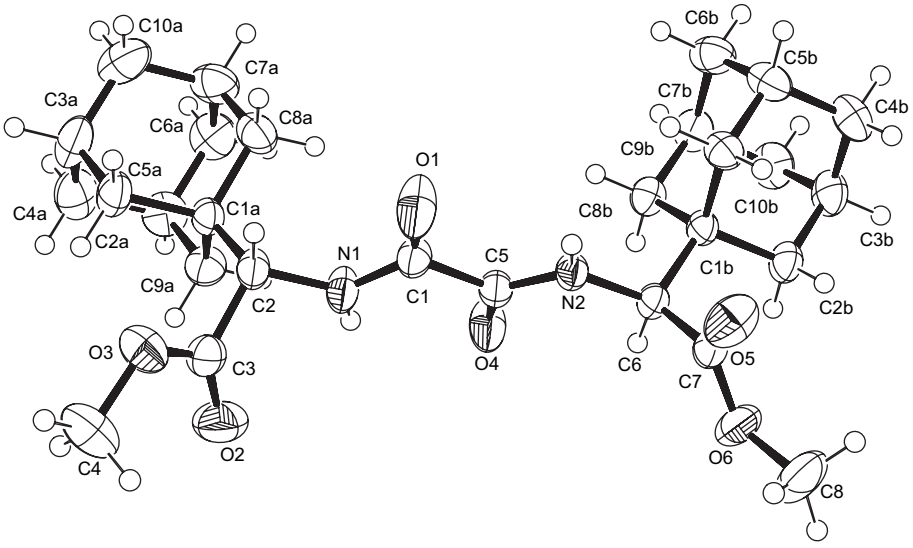

Figure 2. The molecular structure of *rac*-**1** with the atom numbering scheme. Thermal ellipsoids are drawn at the 50% probability level. The molecular symmetry is C_1.

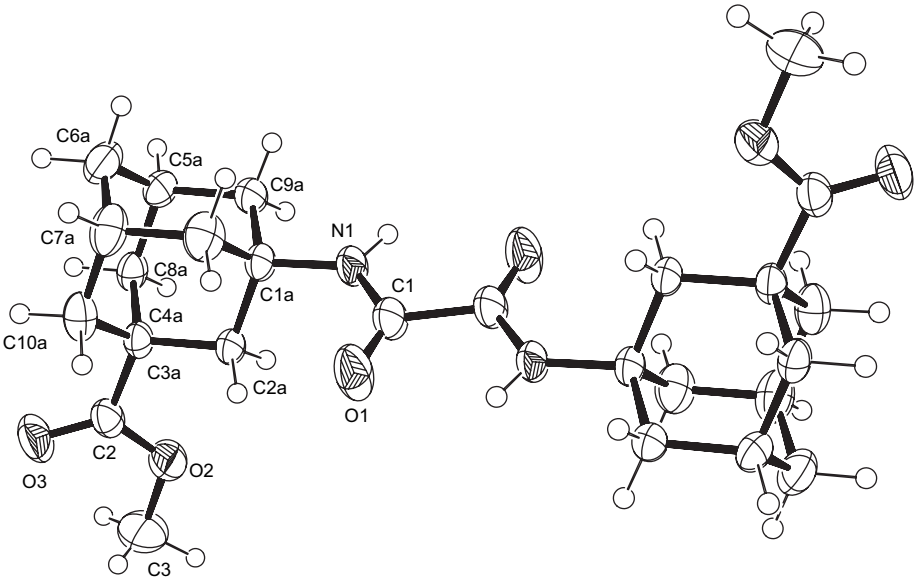

Figure 3. The molecular structure of **2** with the atom numbering scheme. Thermal ellipsoids are drawn at the 50% probability level. The molecular symmetry is C_i.

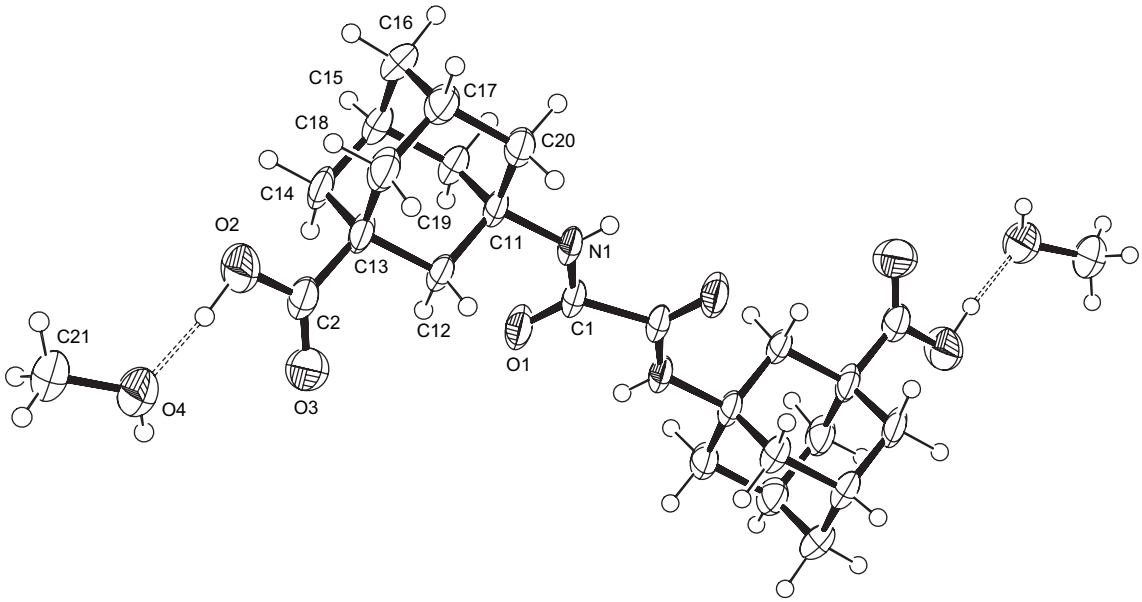

Figure 4. The molecular structure of **3**·MeOH with the atom numbering scheme. Intermolecular hydrogen bond O–H···O connects solvent and the molecule of **3**. Thermal ellipsoids are drawn at the 50% probability level. The molecular symmetry is C_i.

inversion centre located in the middle of the oxalamide bridge) whereas *rac*-**1** (Fig. 2) is chiral and crystallizes as a racemate. In the structure of **3**·EtOAc there are two symmetry-independent molecules, **a** and **b** (Fig. 5), both exhibiting an approximate C_i molecular symmetry. In addition, molecules **a** and **b** are related by a pseudo-inversion centre.

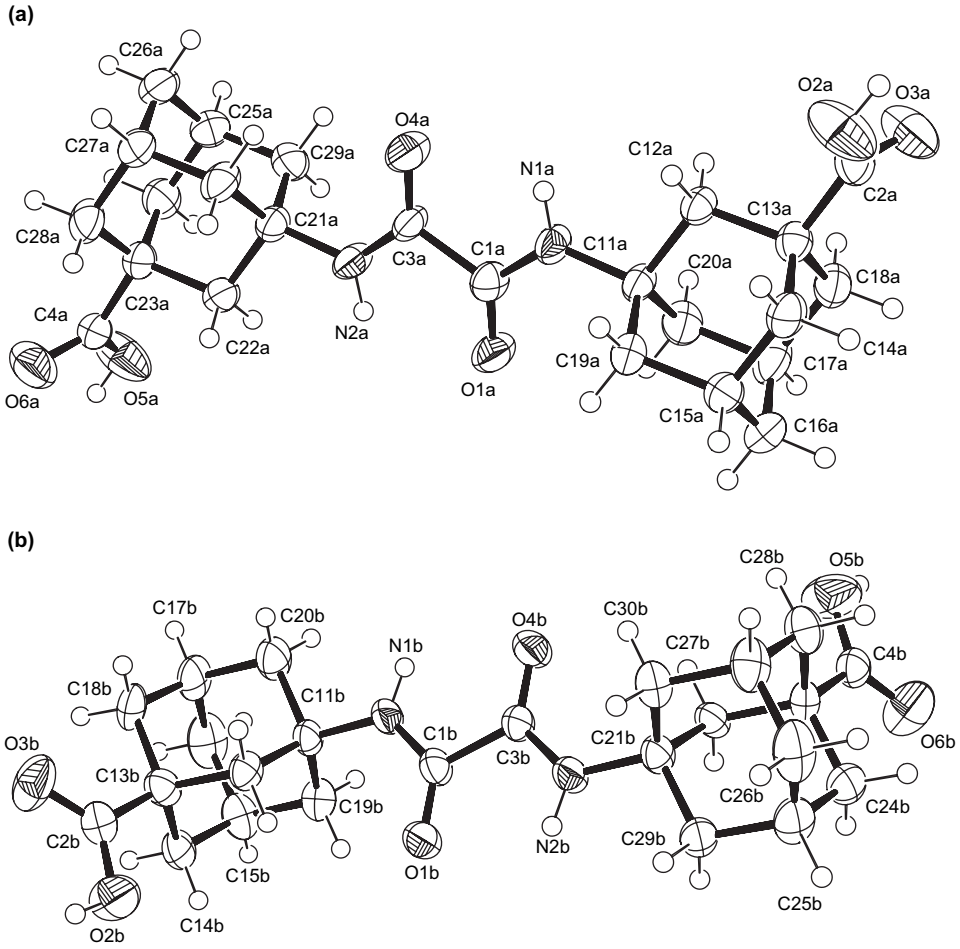

Figure 5. The molecular structures of two symmetry-independent molecules of **3**·EtOAc (labelled as **a** and **b**) with the atom numbering scheme. Thermal ellipsoids are drawn at the 50% probability level. Both molecules have an approximate molecular C_i symmetry.

Table 1. Selected torsion angles (°) defining molecular conformations

Structure		Torsion angle (°)
meso-**1**	C1a–C2–N1–C1	106.9(2)
	C3–C2–N1–C1	−128.4(2)
	C2–N1–C1–C1^{i}	−174.9(2)
	C2–N1–C1–O1	4.6(4)
	N1–C1–C1^{i}–N1^{i}	180.0(2)
	O1–C1–C1^{i}–O1^{i}	180.0(3)
rac-**1**	C1a–C2–N1–C1	−112.9(2)
	C3–C2–N1–C1	123.9(2)
	C2–N1–C1–C5	−177.3(3)
	C2–N1–C1–O1	1.8(3)
	N1–C1–C5–N2	−169.2(2)
	O1–C1–C5–O4	−168.4(2)
	O4–C5–N2–C6	2.9(3)
	C5–N2–C6–C1b	105.8(2)
	C5–N2–C6–C7	−130.1(2)
2	C1a–N1–C1–C1^{i}	178.3(1)
	C1a–N1–C1–O1	−1.9(2)
	N1–C1–C1^{i}–N1^{i}	180.0(1)
	O1–C1–C1^{i}–O1^{i}	180.0(2)
3·MeOH	C11–N1–C1–C1^{i}	−178.6(3)
	C11–N1–C1–O1	0.6(6)
	N1–C1–C1^{i}–N1^{i}	180.0(3)
	O1–C1–C1^{i}–O1^{i}	180.0(3)
3·EtOAc	C11a–N1a–C1a–O1a	3.6(7)
	C11a–N1a–C1a–C3a	−177.7(3)
	N1a–C1a–C3a–N2a	179.5(4)
	O1a–C1a–C3a–O4a	−179.2(4)
	C1a–C3a–N2a–C21a	−178.2(4)
	O4a–C3a–N2a–C21a	1.7(7)
	C11b–N1b–C1b–O1b	1.5(6)
	C11b–N1b–C1b–C3b	179.6(3)
	N1b–C1b–C3b–N2b	179.2(3)
	O1b–C1b–C3b–O4b	−177.5(4)
	C1b–C3b–N2b–C21b	179.1(4)
	O4b–C3b–N2b–C21b	−2.6(7)

Symmetry code: (*i*) −*x*, −*y*, −*z*.

Oxalamide bridges in *meso*-**1**, **2** and **3**·MeOH are planar due to symmetry requirements and hybridization involved: the torsion angles O=C–C=O are 180°. However, the oxalamide bridges are distorted from 180° in the molecule **b** of **3**·**EtOAc** for 2.5(4)° and in *rac*-**1** for 11.6(2)° (Table 1). In the studied retropeptides, the bulky adamantane cages are in *anti* arrangement, as required by the C_i molecular symmetry, however, *rac*-**1** having C_1 molecular symmetry reveals a *syn* orientation. Thus, the steric hindrance imposed by closely positioned adamantane cages and the crystal structural pattern influence bending of the oxalyl bridge. A similar distortion of the oxalamide group (10.8°) was also reported in the case of crystal structure of *N*,*N*′-bis(*S*-valyl)oxalamide, which forms a double helix of hydrogen-bonded chains.[9a]

Crystal packings of *meso*-**1** and *rac*-**1** reveal one-dimensional hydrogen bond network defined by infinite chains of molecules interconnected by N–H···O interactions. In *meso*-**1** (Fig. 6, Table 2), the building units of the hydrogen-bonded chain are two distinctive ring skeletons of $\mathbf{R}_2^2(10)$ topology.[11,12] One is generated by pairs of symmetry-related N1–H···O2 hydrogen bond connecting oxalamide and carboxyl groups whereas the other one involves N1–H···O2 and C4–H···O1 interactions, both generating an infinite chain along the direction [100]. An additional C–H···O hydrogen bond (Table 2) between adamantane methylene group and oxalamide oxygen completes a network. There is no typical 'ladder' pattern[9,13] $\mathbf{C}(4)\mathbf{C}(4)\mathbf{R}_2^2(10)$ that interconnects the oxalamide moieties via N–H···O hydrogen bonds, which are characteristic of a one-dimensional α-network.[8,9b] According to the search of CSD (version 5.28, November 2006)[14] out of 74 observed oxalamide structures, 29 structures reveal

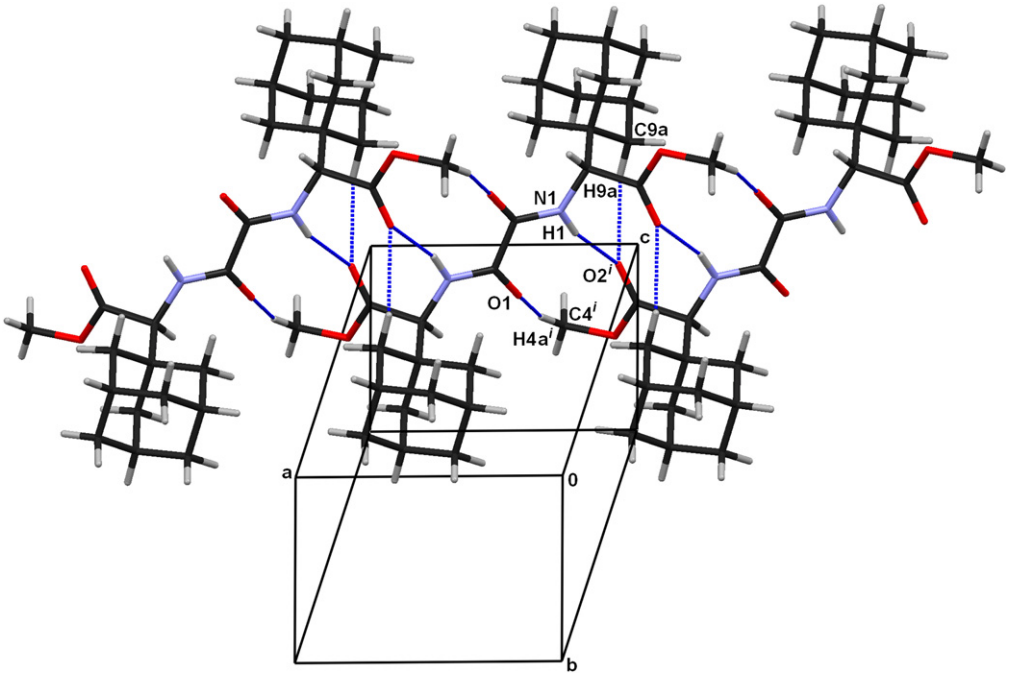

Figure 6. The crystal packing of *meso*-**1** with hydrophilic hydrogen-bonded chain embodied into hydrophobic adamantane layers. Symmetry code: (i) −*x*, −*y*, 2−*z*.

Table 2. Geometrical parameters of hydrogen bonds of *meso*-**1**, *rac*-**1**, **2** and solvates of **3**

Structure	Hydrogen bond	*D*–H /Å	H···*A*/Å	*D*–H···*A*/···	*D*–H···*A*/°	Symm. operation on *A*
meso-**1**	N1–H1···O2	0.90(3)	2.30(3)	3.162(3)	160(2)	$-x, -y, 2-z$
	C4–H4a···O1	1.04(4)	2.34(3)	3.325(4)	158(3)	$1+x, y, z$
	C9a–H9a···O2	1.04(3)	2.50(3)	3.463(3)	154(2)	$-x, -y, 2-z$
	N1–H1···O1[a]	0.90(3)	2.35(3)	2.710(3)	104(2)	$-1-x, -y, 2-z$
rac-**1**	N2–H2n···O1	0.87(2)	2.19(2)	3.056(2)	173.9(16)	$-x, 1-y, 1-z$
	C2–H2···O5	0.98	2.71	3.618(4)	154	$-x, 1-y, 1-z$
	C2b–H2c···O4	0.97	2.72	3.564(4)	146	$-x, -y, 1-z$
	C8b–H8f···O4	0.97	2.56	3.447(2)	152	$-x, -y, 1-z$
	N1–H1n···O4[a]	0.82(2)	2.24(2)	2.647(2)	111.3(19)	x, y, z
	N2–H2n···O1[a]	0.87(2)	2.41(2)	2.761(2)	105.0(15)	x, y, z
2	N1–H1n···O3	0.895(17)	2.286(17)	3.136(2)	158.6(15)	$x, -1+y, z$
	C3–H3b···O3	1.01(3)	2.66(3)	3.626(3)	161(2)	$1-x, 2-y, 2-z$
	C9a–H9a···O3	0.984(16)	2.587(16)	3.163(2)	117.5(12)	$x, -1+y, z$
	N1–H1n···O1[a]	0.895(17)	2.240(16)	2.6902(19)	110.7(13)	$1-x, -y, 1-z$
3·MeOH	O2–H2···O4	0.99(5)	1.65(5)	2.628(7)	175(3)	x, y, z
	O4–H4···O1	0.85(5)	1.95(6)	2.788(7)	166(9)	$1/2+x, 1/2-y, 1/2+z$
	N1–H1···O3	0.79(5)	2.60(5)	3.346(8)	158(5)	$1/2-x; -1/2+y; 1/2-z$
	C20–H20a···O3	1.09(5)	2.65(5)	3.220(8)	112(3)	$1/2-x, -1/2+y, 1/2-z$
	C21–H21a···O3	0.95(3)	2.64(4)	3.581(7)	169(4)	$1/2+x, 1/2-y, 1/2+z$
	N1–H1···O1[a]	0.79(5)	2.36(6)	2.690(6)	107(5)	$-x, -y, -z$
3·EtOAc	N1a–H1a···O4b	0.86	2.48	3.117(6)	131	$-1+x, y, z$
	N1b–H1b···O4a	0.86	2.46	3.175(6)	141	$1+x, y, z$
	N2a–H2a···O1b	0.86	2.48	3.121(6)	132	x, y, z
	N2b–H2b···O1a	0.86	2.45	3.171(6)	142	x, y, z
	O2a–H3a···O6b	0.82	1.83	2.648(6)	172	$-1+x, -1+y, z$
	O2b–H3b···O6a	0.82	1.80	2.613(6)	172	$x, -1+y, z$
	O5a–H5a···O3b	0.82	1.80	2.614(6)	171	$x, 1+y, z$
	O5b–H5b···O3a	0.82	1.84	2.655(6)	173	$1+x, 1+y, z$
	C12a–H12b···O4b	0.97	2.64	3.457(7)	142	$-1+x, -1+y, z$
	C20b–H20b···O4a	0.97	2.58	3.358(7)	137	$1+x, y, z$
	C22a–H22a···O1b	0.97	2.67	3.477(7)	141	x, y, z
	C29b–H29d···O1a	0.97	2.58	3.350(7)	137	x, y, z
	N1a–H1a···O4a[a]	0.86	2.26	2.670(5)	109	x, y, z
	N2a–H2a···O1a[a]	0.86	2.26	2.677(5)	110	x, y, z
	N1b–H1b···O4b[a]	0.86	2.29	2.704(5)	110	x, y, z
	N2b–H2b···O1b[a]	0.86	2.26	2.678(5)	110	x, y, z

[a] Intramolecular pseudo-C_5 hydrogen bond is analogous to the C_5 in peptides. Crystallographically independent molecules are marked by **a** and **b**.

no interaction between the oxalamide moieties. In such cases, the most frequent motif is $\mathbf{R}_2^2(n)$, rings with n being 8–12, as detected in the structure of *meso*-**1**. Bulky adamantane cages obstruct oxalamide···oxalamide hydrogen bonds; therefore, the oxalamide group acts as a proton donor to an ester O (sp^2) generating a hydrogen-bonded ring with graph-set symbol $\mathbf{R}_2^2(10)$.

Molecules of *rac*-**1** form centrosymmetric dimers by pairs of symmetry-related N2–H···O1 between oxalamide bridges generating rings with $\mathbf{R}_2^2(10)$ topology. Additionally, C2–H···O5 supports dimer formation. Two pairs of symmetry-related C–H···O hydrogen bonds (Fig. 7, Table 2) connect dimers into infinite chains parallel to the direction [010]. The hydrogen-bonded dimer of $\mathbf{R}_2^2(10)$ topology observed in *rac*-**1** is also detected in the two structures, *N*,*N*′-oxalyl-bis(valine)retropeptide[9b] and catena(diaqua-2,2′-bipyridyl-(μ_2-oxalamide-*N*,*N*′-di-3-propionato-*O*,*O*′)-copper(II) monohydrate)[15] in CSD.[14]

In compound **2** (Fig. 8) pairs of symmetry-related N1–H···O3 and C9a–H···O3 hydrogen bonds connect molecules into infinite chains parallel to the direction [001]. The weak hydrogen bond C3–H···O3 links the chains into layers parallel to the plane (100) (Table 2). The alternating hydrophilic and hydrophobic regions are running along [001].

In spite of the efforts to obtain crystals of **3**, only solvates were crystallized. In the methanol solvate (**3**·MeOH), both oxalamide and carboxyl moieties are hydrogen bonded by O–H···O to the methanol molecule forming rings of $\mathbf{R}_3^3(11)$ topology (Fig. 9). Each molecule of **3**·MeOH participates in formation of four symmetry-related rings generating layers parallel to the plane (10−1) (Fig. 9). In the crystal structure of the ethyl acetate solvate (**3**·EtOAc), two distinctive intermolecular hydrogen-bonding motifs are present. Oxalamide moieties of two symmetrically independent molecules **a** and **b** are interconnected by hydrogen bonds N–H···O forming ribbons of $\mathbf{C}(4)\mathbf{C}(4)\mathbf{R}_2^2(10)$ topology; typical oxalamide 'ladder' patterns[9b,13,14] occur (Fig. 10a). They extend in the direction [100]. The hydrogen-bonded carboxyl groups of molecules **a** and **b** form eight-membered rings $\mathbf{R}_2^2(8)$; this hydrogen-bonded motif is typical of carboxylic acids.[14,16,17] They link molecules into double chains parallel to the direction [110] (Fig. 10b) forming a channel-like structure (Fig. 10c). The channels extending in the direction [100] are filled with ethyl acetate molecules (Fig. 10c). Interestingly, the solvent molecules do not participate in hydrogen bonds at all.

The crystal packing of retropeptides having oxalyl bridges and adamantyl groups in the terminal positions optimizes the

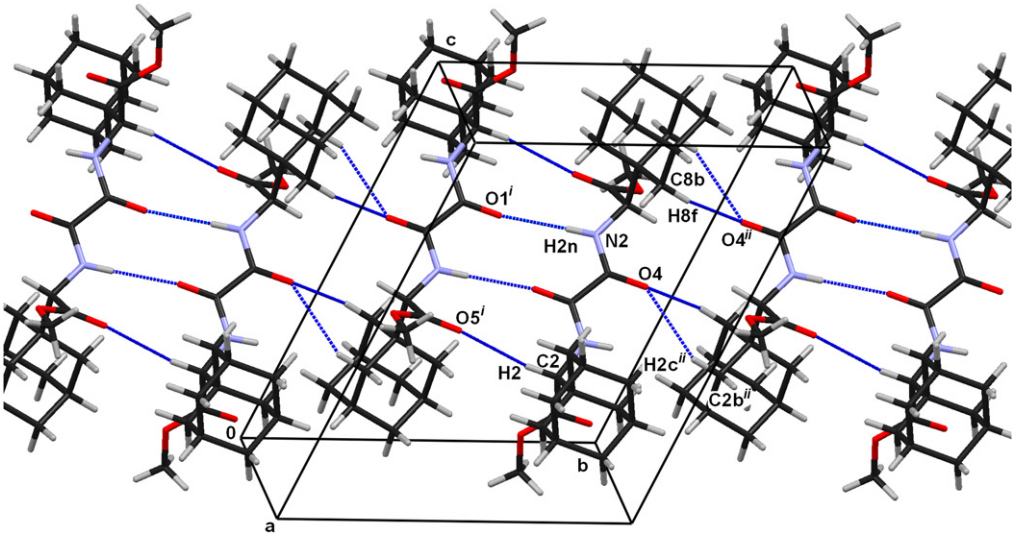

Figure 7. The crystal packing of *rac*-**1** having pronounced separation of hydrophilic region by hydrogen-bonded rings connected into chains, and adamantane hydrophobic layers. Symmetry codes: (i) $-x$, $1-y$, $1-z$; (ii) $-x$, $-y$, $1-z$.

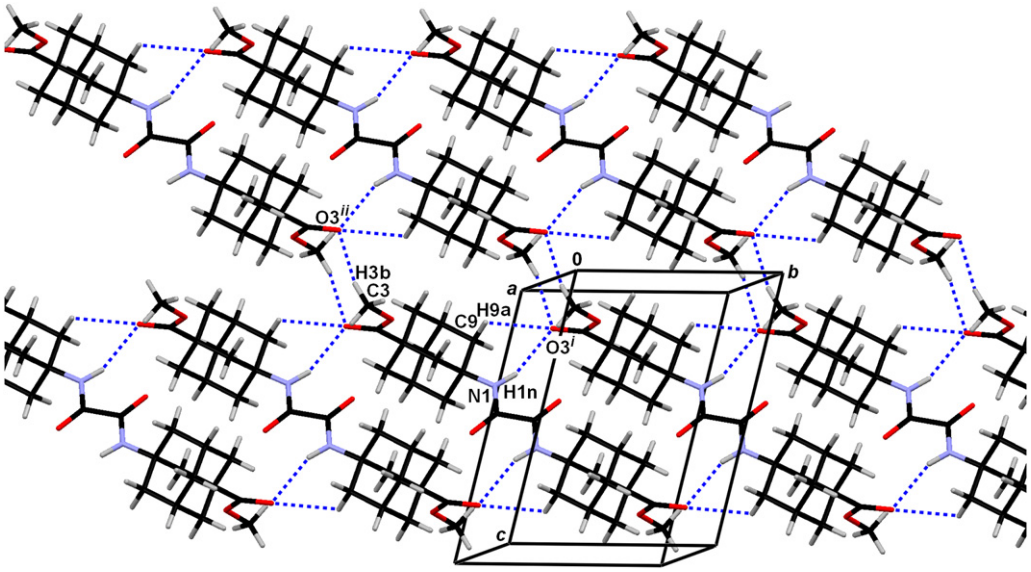

Figure 8. The crystal packing of **2** with two-dimensional hydrogen-bonding network in the plane (101) separated by hydrophobic adamantane cages. Symmetry codes: (i) x, $-1+y$, z; (ii) $1-x$, $2-y$, $2-z$.

influences of chirality and steric hindrance (bulky adamantyl group). The compounds *meso*-**1** and *rac*-**1** having chiral centres in the crystals exhibit one-dimensional α-networks of hydrogen bonding[8] (Figs. 6 and 7). In both crystal structures hydrogen-bonded molecules are related by an inversion symmetry operation generating *meso*-layers. In *meso*-**1** molecular fractions of different chirality are connected into a *meso*-layer whereas in *rac*-**1** hydrogen-bonded enantiomers *R* and *S* form *meso* hydrophilic layer (Fig. 7). In the crystals, however, achiral **2**, **3**·MeOH and **3**·EtOAc generate the two-dimensional hydrogen-bonded β-network[8] with alternating hydrophobic and hydrophilic layers (Figs. 8–10).

In the crystal packing of **3**·MeOH, methanol, as a protic and highly polar solvent, acts as proton donor to the oxalyl oxygen and an acceptor to the OH group of carboxyl moiety. On the contrary, in **3**·EtOAc, the aprotic solvent, ethyl acetate, does not participate in hydrogen bonding at all. Hydrogen-bonded oxalamide···oxalamide and carboxyl··· carboxyl groups of two symmetrically independent molecules generate the two-dimensional network with channels accommodating ethyl acetate molecules. By the selection of a solvent molecule of appropriate polarity and size, one can design the crystal packing.

3. Conclusions

Novel adamantane-oxalamide derivatives, *meso*-**1**, *rac*-**1**, **2** and **3** were prepared in a single step by direct condensation of oxalyl chloride and the corresponding adamantane derivatives. Their chemical and physical properties were

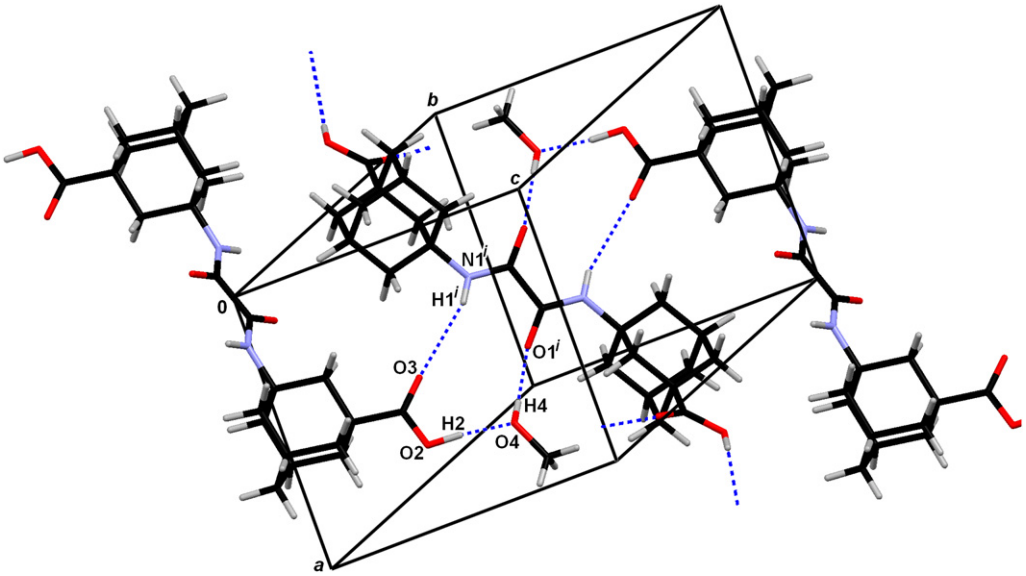

Figure 9. The crystal packing of **3**·MeOH involves the two-dimensional hydrogen-bonding network. The alternating hydrophilic and hydrophobic regions characterize the β-network. Symmetry code: (i) ½+*x*, ½−*y*, ½+*z*.

investigated by spectroscopic methods and X-ray structural analysis. The crystal packings of the studied derivatives are different. Whereas bulkiness of adamantanes does not allow formation of the β-network in *meso*-**1** and *rac*-**1**, this type of self-assembly was feasible in the oxalamides **2** and **3**. Retropeptides *meso*-**1** and *rac*-**1** self-assemble into structures, which are governed by one-dimensional α-networks of hydrogen bonds. The ester derivatives of oxalamides *meso*-**1**, *rac*-**1** and **2** as well as diacid derivative **3** showed no tendency to form gels with organic solvents or water. The bulky adamantane substituent prevents oxalamide···oxalamide hydrogen bonding. Thus, imposed steric requirements of adamantane cages prevent the reorganization of self-assembled molecules, which is needed for gelation in order to release space for solvent molecules to be trapped. The oxalamide **3** crystallizes in the form of solvates. The protic solvent (MeOH) incorporates into the crystal structure participating in the hydrogen bonding between the oxalamide and carboxyl moieties. On the other hand, non-protic solvent (EtOAc) does not participate in hydrogen bonding. The crystal packing of **3**·EtOAc showed a two-dimensional network with channels that can accommodate EtOAc molecules. To the best of our knowledge, this is the first example of such a packing of oxalamides. Knowledge of the packing pattern of adamantane-oxalamides may be useful for the supramolecular synthesis of new materials characterized by the presence of nanochannels of different size and geometry.

4. Experimental

4.1. General

^{1}H and ^{13}C NMR spectra were recorded on a Bruker AV-300 or 600 Spectrometer at 300 or 600 MHz, respectively. All NMR spectra were measured in $CDCl_3$ or DMSO-d_6 using tetramethylsilane as a reference. The assignment of the signals is based on two-dimensional homonuclear correlated spectroscopy (COSY) and heteronuclear multiple quantum coherence (HMQC). High-resolution mass spectra (HRMS) were measured on an Extrel FTMS 2001 DD using electron impact ionization mode. Melting points were obtained using an Original Kofler Mikroheitztisch apparatus (Reichert, Wien) and are uncorrected. Silica gel (Merck 0.05–0.2 mm) was used for chromatographic purifications. Solvents were purified by distillation. Adamantane amino acids: (1-adamantyl)glycine (**4**)[6,10a] and 3-aminoadamantane-1-carboxylic acid (**5**)[6,10b,c] were prepared according to the procedure described in literature.

4.2. 3-Aminoadamantane-1-carboxylic acid methyl ester (7)

In a round bottom flask 1.00 g of amino acid hydrochloride **5** was dissolved in 50 mL of dry methanol (molecular sieves 3 Å). The solution was cooled to −5 °C and 1 mL of thionylchloride was added. After stirring at −5 °C over 15 min, the reaction was stirred at rt for an h and heated at temperature of reflux for 24 h. The solvent was removed and to the residue 50 mL of saturated aqueous solution of $NaHCO_3$ was added. Extractions with dichloromethane were carried out (4× 25 mL) and collected extracts were dried over anhydrous $MgSO_4$. After filtration and evaporation of the solvent, crude ester was obtained (900 mg, ~99%) and was used in the next step without further purification. For the purpose of analysis, a small amount of ester **7** was purified by column chromatography on silica gel using CH_2Cl_2/CH_3OH (up to 5%) as eluent.

Ester **7**: oily solid, mp ~20 to 25 °C; IR (KBr) ν 2909 (NH), 1727 (CO); ^{1}H NMR ($CDCl_3$, 600 MHz) δ 3.58 (s, 3H, OCH_3), 2.10 (br s, 2H), 1.73 (d, 2H, J=12.3 Hz), 1.67 (d, 2H, J=12.3 Hz), 1.63 (s, 2H), 1.56 (br s, 2H, NH), 1.40–1.55 (m, 6H); ^{13}C NMR ($CDCl_3$, 150 MHz) δ 176.98 (s), 51.34 (q), 47.35 (s), 47.12 (t), 44.72 (t), 42.72 (s), 37.51 (t), 34.89 (t), 29.14 (d); MS (*m*/*z*) 210 (M+H^{+}, 60), 153 (75), 151 (60), 120 (30), 94 (100); HRMS calcd for $C_{12}H_{20}NO_2$: 210.1489, found: 210.1485.

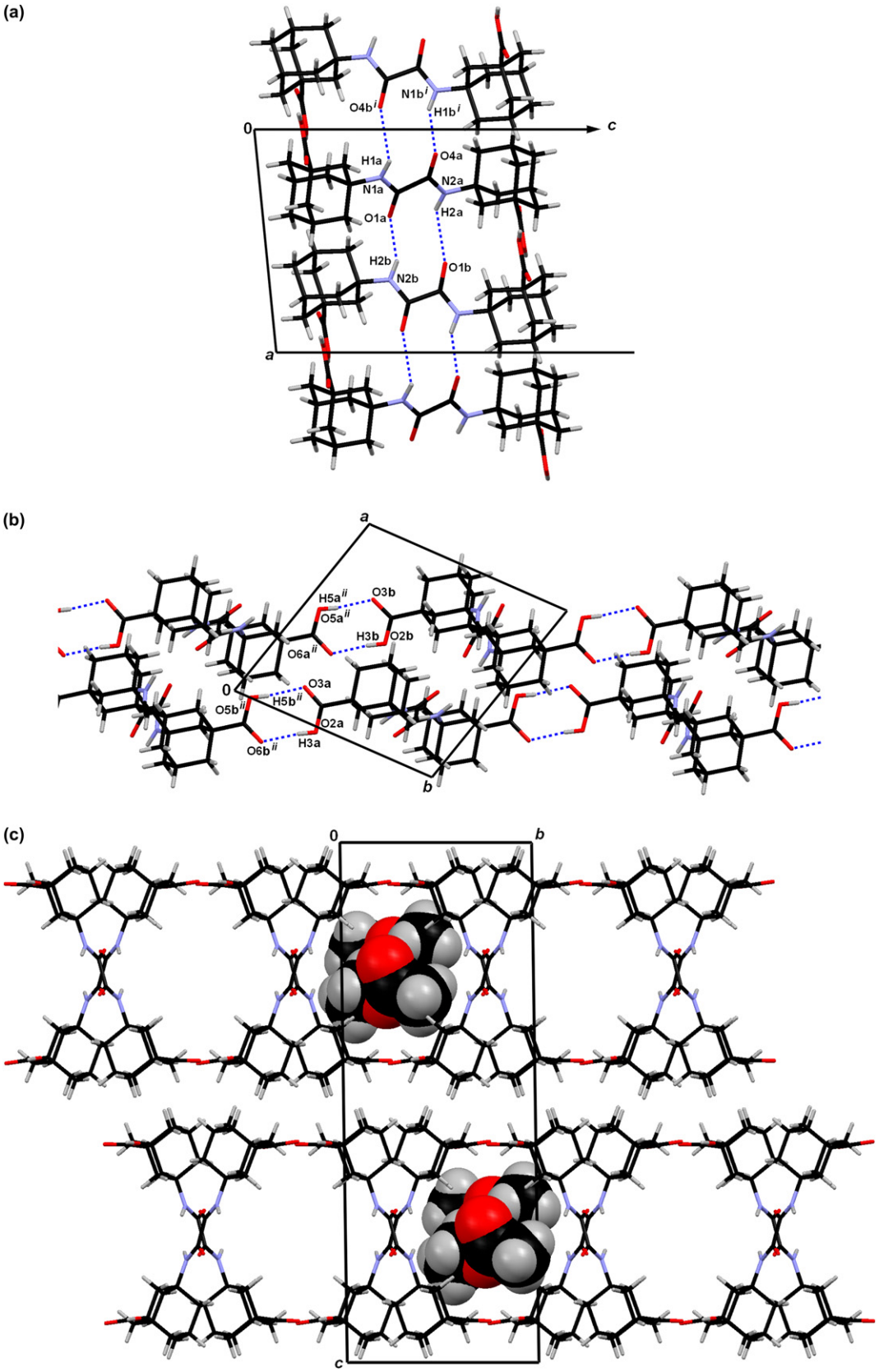

Figure 10. The crystal packing of **3**·EtOAc with the two-dimensional hydrogen-bonding network: (a) hydrogen-bonded chains between oxalamide moieties extending in the direction [100]; (b) hydrogen bonds connecting carboxyl groups form chains extended in the direction [110]; (c) double layers parallel to [001] with solvent-filled channels running parallel to the direction [100]. Solvent molecules are drawn within the frame of the unit cell whereas other channels are left blank to emphasize the channels in the crystal packing. Symmetry codes: (i) $-1+x, y, z$; (ii) $x, -1+y, z$.

4.3. Preparation of *N,N′*-bisoxalamide derivatives: general procedure

In a round bottom flask under a stream of N_2 was placed 1 equiv of amino acid methyl ester (**6** or **7**) and dissolved in 10 mL of dry CH_2Cl_2. To the solution, dry triethylamine (1.5–2 mL) was added. The reaction mixture was cooled to −5 °C and to the cooled solution under N_2, half an equivalent of oxalyl chloride was added in several portions by use of a syringe. The reaction mixture was stirred at −5 °C for 1 h, allowed to reach rt and stirred at rt for 2 days. After 2 days, reaction mixture was diluted by the addition of 50 mL of CH_2Cl_2 and washed with 5% aqueous solution of acetic acid (3×50 mL) followed by washing with saturated aqueous $NaHCO_3$ (3×50 mL). The organic layer was dried over anhydrous $MgSO_4$ and filtered. The solvent was removed on a rotary evaporator to furnish crude product.

4.3.1. *N,N′*-Bis(1-adamantylglycine methyl ester)oxalamide (1). The reaction was carried out starting from 250 mg (1.12 mmol) of hydrochloride of **6**[6] and 49 μL (0.56 mmol) of oxalyl chloride in the presence of 0.5 mL of triethylamine to yield 270 mg (98%) of the crude product. Reaction yielded a mixture of diastereomers in a ratio of 1:1, which were separated on a thin layer of silica gel using CH_2Cl_2 as a solvent [*meso*-**1**: R_f (CH_2Cl_2)=0.36; *rac*-**1**: R_f (CH_2Cl_2)=0.20].

Oxalamide *meso*-**1**: colourless crystals (acetone/CH_2Cl_2/$CHCl_3$=200:10:3), mp 238–241 °C; IR (KBr) ν 3337 (NH), 2903 (CH), 1737 (CO-ester), 1677 (CO-amide); ^{1}H NMR ($CDCl_3$, 300 MHz) δ 7.86 (d, 2H, J=9.9 Hz, NH), 4.27 (d, 2H, J=9.9 Hz, CH-gly), 3.75 (s, 6H, OCH_3), 2.00 (br s, 6H, H-ad), 1.50–1.75 (m, 24H, H-ad); ^{13}C NMR ($CDCl_3$, 75 MHz) δ 169.92 (s, CO-ester), 158.91 (s, CO-amide), 61.44 (d, CH-gly), 51.78 (q, OCH_3), 38.46 (t, ad), 36.72 (s, ad), 36.36 (t, ad), 28.01 (d, ad); MS (*m/z*) 501 (M+H$^+$, 80), 135 (100); HRMS calcd for $C_{28}H_{41}N_2O_6$: 501.2959, found: 501.2962.

Oxalamide *rac*-**1**: colourless crystals (acetone/CH_2Cl_2/$CHCl_3$=12:3:2), mp 215–218 °C; IR (KBr) ν 3399 (NH), 3291 (NH), 2906 (CH), 1736 (CO-ester), 1676 (CO-amide); ^{1}H NMR ($CDCl_3$, 300 MHz) δ 7.84 (d, 2H, J=9.8 Hz, NH), 4.25 (d, 2H, J=9.8 Hz, CH-gly), 3.74 (s, 6H, OCH_3), 2.02 (br s, 6H, H-ad), 1.55–1.75 (m, 24H, H-ad); ^{13}C NMR ($CDCl_3$, 75 MHz) δ 169.85 (s, CO-ester), 159.05 (s, CO-amide), 61.54 (d, CH-gly), 51.77 (q, OCH_3), 38.48 (t, ad), 36.46 (s, ad), 36.35 (t, ad), 28.00 (d, ad).

4.3.2. *N,N′*-Bis(3-aminoadamantane-1-carboxylic acid methyl ester)oxalamide (2). The reaction was carried out starting from 700 mg (3.35 mmol) of **7** and 150 μL (1.67 mmol) of oxalyl chloride to yield 750 mg (94%) of the crude product **2**, which was purified by recrystallization using CH_2Cl_2 as a solvent.

Oxalamide **2**: colourless crystals (CH_2Cl_2), mp 215–216 °C; IR (KBr) ν 3318 (NH), 2918 (CH), 1719 (CO-ester), 1678 (CO-amide); ^{1}H NMR ($CDCl_3$, 600 MHz) δ 7.25 (br s, 2H, NH), 3.58 (s, 6H, OCH_3), 2.16 (br s, 4H), 2.10 (s, 4H), 1.95 (d, 4H, J=11.3 Hz), 1.86 (d, 4H, J=11.3 Hz), 1.78 (s, 8H), 1.45–1.65 (m, 4H); ^{13}C NMR ($CDCl_3$, 150 MHz) δ 176.40 (s), 159.03 (s), 51.82 (s), 51.53 (q), 42.24 (s), 41.44 (t), 39.85 (t), 37.52 (t), 34.91 (t), 28.71 (d); MS (*m/z*) 473 (M+H$^+$, 60), 193 (100); HRMS calcd for $C_{26}H_{37}N_2O_6$: 473.2646, found: 473.2650.

4.4. Ester hydrolysis: general procedure

In a round bottom flask was placed ~300 to 500 mg of the ester derivatives **1** or **2**, and a mixture of CH_3OH (10 mL) and 10% aqueous Na_2CO_3 (20 mL) was added. The mixture was heated at the temperature of reflux for 2 days until the solid was completely dissolved. The cooled reaction mixture was washed with CH_2Cl_2 (3×25 mL) and the aqueous layer acidified with 1 M HCl until it reached pH 2. The acidic mixture was extracted with ethyl acetate (4×25 mL), extracts were dried over anhydrous $MgSO_4$, filtered and the solvent was removed under reduced pressure to afford the crude product.

*N,N′-Bis(3-aminoadamantane-1-carboxylic acid)oxalamide (**3**)* was obtained by hydrolyzing 500 mg (1.06 mmol) of **2**. The crude product (370 mg, 79%) was purified by recrystallization using methanol as a solvent.

Oxalamide **3**: colourless crystals (CH_3OH), mp >310 °C; IR (KBr) ν 3000–3600 (COOH), 2939 (CH), 1719 (CO-acid), 1665 (CO-amide); ^{1}H NMR (DMSO-d_6, 300 MHz) δ 12.00 (br s, 2H, COOH), 7.75 (br s, 2H, NH), 2.12 (br s, 4H), 2.05 (br s, 4H), 1.96 (d, 4H, J=11.9 Hz), 1.87 (d, 4H, J=11.9 Hz), 1.72 (br s, 8H), 1.50–1.60 (m, 4H); ^{13}C NMR (DMSO-d_6, 75 MHz) δ 177.03 (s), 159.02 (s), 51.36 (s), 41.31 (t), 41.27 (s), 39.36 (t), 37.32 (t), 34.61 (t), 28.30 (d); MS (*m/z*) 445 (M+H$^+$, 30), 399 (30) 357 (60), 196 (60), 179 (100), 161 (40), 133 (40); HRMS calcd for $C_{24}H_{33}N_2O_6$: 445.2333, found: 445.2330.

The mixture of stereoisomers of N,N′-bis(1-adamantylglycine)oxalamide was obtained from 270 mg of the mixture of esters *rac*-**1** and *meso*-**1**. The reaction furnished 50 mg (20%) of the mixture of the diacid diastereomers, which was hardly soluble in most of the solvents (only slightly in alcohols and EtOAc) and therefore difficult to separate and purify. ^{1}H NMR (DMSO-d_6, 300 MHz) δ 12.5 (br s, 2H, COOH), 7.92–8.00 (br s, 2H, NH), 3.96–4.00 (m, 2H, CH), 1.96 (br s, 6H), 1.50–1.70 (m, 24H); ^{13}C NMR (DMSO-d_6, 75 MHz) δ 172.93 (s, COO-1), 170.69 (s, COO-2), 159.11 (s, CONH-1), 158.89 (s, CONH-2), 61.47 (d, CH-1), 61.32 (d, CH-2), 34.0–39.0 (2×ad 1s, 2t), 27.77 (d, C-ad-1), 27.68 (d, C-ad-2). MS (*m/z*) 471 (M−H$^+$, 20), 425 (20), 281 (70), 280 (100); HRMS calcd for $C_{26}H_{35}N_2O_6$: 471.2500, found: 471.2503.

5. Crystallography

The single crystals of the oxalamides *meso*-**1**, *rac*-**1**, **2** and **3** were obtained by slow evaporation of the mixture of solvents acetone/CH_2Cl_2/$CHCl_3$=200:10:3 (*meso*-**1**), acetone/CH_2Cl_2/$CHCl_3$=12:3:2 (*rac*-**1**), CH_2Cl_2 (**2**) and CH_3OH or ethyl acetate (**3**), respectively. The methanol solvate (**3**·MeOH) decays in air, losing the solvent molecules within several days. The room-temperature structure, although poor due to gradual decomposition of the crystals during the data

Table 3. Crystallographic data and structural refinement data for the crystal structures of *meso*-**1**, *rac*-**1**, **2**, **3**·MeOH and **3**·EtOAc

Compound	*meso*-**1**	*rac*-**1**	**2**	**3**·MeOH	**3**·EtOAc
Empirical formula	$C_{28}H_{40}N_2O_6$	$C_{28}H_{40}N_2O_6$	$C_{26}H_{36}N_2O_6$	$C_{26}H_{40}N_2O_8$	$C_{28}H_{40}N_2O_8$
Formula wt./gmol^{-1}	500.62	500.62	472.57	508.60	532.62
Crystal dimensions/mm	0.25×0.18×0.10	0.29×0.20×0.08	0.20×0.20×0.15	0.30×0.20×0.10	0.30×0.12×0.12
Space group	$P-1$	$P-1$	$P-1$	$P2_1/n$	$P-1$
a/Å	7.7292(7)	8.9634(5)	7.1677(5)	9.378(6)	10.2482(10)
b/Å	8.5884 (6)	10.9877(6)	7.9060(4)	10.40(2)	10.2611(12)
c/Å	10.7116(8)	14.6301(7)	11.0085(3)	13.55(2)	27.00(3)
α/°	75.003(6)	68.194(4)	104.690(3)	90	87.60 (6)
β/°	88.137(7)	75.594(4)	94.530(4)	108.90(10)	83.92(6)
γ/°	76.271(7)	86.838(4)	98.980(5)	90	74.536(8)
Z	1	2	1	2	4
V/Å^3	666.89(10)	1294.60(12)	591.43(6)	1250(3)	2721(3)
D_{calcd}/g cm^{-3}	1.247	1.284	1.327	1.351	1.30
μ/mm^{-1}	0.707	0.728	0.653	0.823	0.782
θ range/°	4.27–76.24	3.36–76.48	4.18–76.09	5.06–77.65	1.65–76.45
Range of h, k, l	$-9>h>9$, $-10>k>0$, $-13>l>13$	$-11>h>11$, $0>k>13$, $-17>l>18$	$-9>h>8$, $0>k>9$, $-13>l>13$	$-11>h>11$, $-13>k>0$, $-17>l>17$	$0>h>12$, $-12>k>12$, $-33>l>34$
Reflections collected	2885	5719	2638	5060	11,998
Independent reflections	2698	5424	2454	2578	11,341
Observed reflections ($I\geq 2\sigma$)	1706	3810	2073	1702	5089
R_{int}	0.0643	0.0241	0.0109	0.1428	0.0422
$R(F)I>2\sigma(I)$	0.0528	0.0435	0.0388	0.0997	0.0797
$R_w(F^2)I>2\sigma(I)$	0.161	0.1185	0.1075	0.3157	0.3108
Goodness of fit	1.001	1.019	1.066	1.074	1.087
No. of parameters	244	334	227	244	685
$\Delta\rho_{max}$, $\Delta\rho_{min}$ (eÅ^{-3})	0.197, −0.226	0.20, −0.169	0.218, −0.139	0.504, −0.491	0.383, −0.487

collection, was nevertheless good enough to show packing patterns and the hydrogen-bonding scheme. Another type of problem was encountered with the ethyl acetate solvate (**3**·EtOAc). The solvent molecules, which do not participate in hydrogen bonding, displayed large thermal motion. Their geometries and atomic displacement parameters were held rigid in the first few cycles of refinement, but the restraints were released in the latter stage of the refinement, to obtain more reasonable geometric parameters. The C–C bond lengths in molecules of ethyl acetate were restrained to 1.50(1) Å, only. Since both structures, **3**·MeOH and **3**·EtOAc, showed no unreasonable geometric parameters, data collection was not repeated at low temperature. The crystal structure of **3**·EtOAc comprises two molecules in asymmetric units; each of them has an approximate C_i molecular symmetry. These two molecules are related by pseudo-inversion symmetry. The distribution of E-values reveals the hypercentric symmetry.

Data collections were performed on an Enraf Nonius CAD4 diffractometer, using a graphite monochromated Cu Kα (1.54179 Å) radiation at rt [293(2) K]. The WinGX standard procedure was applied for data reduction.[18] Three standard reflections were measured every 120 min as intensity control. The absorption correction based on 8ψ-scan reflections[19] was performed for structures **2** and *rac*-**1**. No absorption correction was applied for structures *meso*-**1**, **3**·MeOH and **3**·EtOAc. The structure was solved with SHELXS97[20] and refined with SHELXL97.[21] The models were refined using the full matrix least squares refinement. Hydrogen atoms were located from difference Fourier maps and refined as free entities for *meso*-**1**, **2** and **3**·MeOH and as mixed free and riding entities for *rac*-**1**. For structure **3**·EtOAc, due to the inferior quality of the measured data, hydrogen atoms were generated at positions expected by stereochemistry and refined as riding entities. The atomic scattering factors were those included in SHELXL97.[21] Molecular geometric calculations were performed with PLATON98,[22] and molecular graphics were prepared using ORTEP-3,[23] and CCDC-Mercury.[24] Crystallographic and refinement data for structures *meso*-**1**, *rac*-**1**, **2**, **3**·MeOH and **3**·EtOAc are shown in Table 3.

Acknowledgements

We thank the Ministry of Science, Education and Sports of the Republic of Croatia for financing (grants no. 098-0982933-2911 and 098-1191344-2943). We also thank Dr. Milan Jokić for the help in gelling experiments.

Supplementary data

Supplementary crystallographic data for this paper can be obtained free of charge via www.ccdc.cam.ac.uk/conts/retrieving.html (or from the Cambridge Crystallographic Data Centre, 12 Union Road, Cambridge CB2 1EZ, UK; fax: +44 1223 336033; or deposit@ccdc.cam.ac.uk). CCDC: 635479–635483 contain the supplementary crystallographic data for this paper. Supplementary data associated with this article can be found in the online version, at doi:10.1016/j.tet.2007.05.066.

References and notes

1. (a) Loughlin, W. A.; Tyndall, J. D. A.; Glenn, M. P.; Fairlie, D. P. *Chem. Rev.* **2004**, *104*, 6085–6117; (b) Becerril, J.; Burguete, M. I.; Escuder, B.; Galindo, F.; Gavara, R.; Miravet, J. F.; Luis, S. V.; Peris, G. *Chem.—Eur. J* **2004**, *10*, 3879–3890; (c) Li, P.; Roller, P. P.; Xu, J. *Curr. Org. Chem.* **2002**, *6*, 411–440; (d) Ojima, I.; Delaloge, F. *Chem. Soc. Rev.* **1997**, *26*, 377–386; (e) Hanessian, S.; McNaughton-Smith,

G.; Lombart, H. G.; Lubell, W. D. *Tetrahedron* **1997**, *53*, 12789–12854; (f) Haubner, R.; Finsinger, D.; Kessler, H. *Angew. Chem., Int. Ed.* **1997**, *36*, 1374–1389; (g) Nowick, J. S.; Smith, E. M.; Parish, M. *Chem. Soc. Rev.* **1996**, *25*, 401–415; (h) Gante, J. *Angew. Chem., Int. Ed. Engl.* **1994**, *33*, 1699–1720; (i) Giannis, A.; Kolter, T. *Angew. Chem., Int. Ed. Engl.* **1993**, *32*, 1244–1267.

2. (a) Ranganathan, D.; Thomas, A.; Haridas, V.; Kurur, S.; Madhusudanan, K. P.; Roy, R.; Kunwar, A. C.; Sarma, A. V. S.; Vairamani, M.; Sarma, K. D. *J. Org. Chem.* **1999**, *64*, 3620–3629; (b) Ranganathan, D.; Haridas, V.; Kurur, S.; Nagaraj, R.; Bikshapathy, E.; Kunwar, A. C.; Sarma, A. V. S.; Vairamani, M. *J. Org. Chem.* **2000**, *65*, 365–374; (c) Ranganathan, D.; Haridas, V.; Nagaraj, R.; Karle, I. L. *J. Org. Chem.* **2000**, *65*, 4415–4422; (d) Davies, J. S. *J. Pept. Sci.* **2003**, *9*, 471–501.
3. (a) Ghadiri, M. R.; Granja, J. R.; Milligan, R. A.; Mcree, D. E.; Khazanovich, N. *Nature* **1993**, *366*, 324–327; (b) Kim, H. S.; Hartgerink, J. D.; Ghadiri, M. R. *J. Am. Chem. Soc.* **1998**, *120*, 4417–4424; (c) Ranganathan, D.; Lakshmi, C.; Haridas, V.; Gopikumar, M. *Pure Appl. Chem.* **2000**, *72*, 365–372; (d) Wang, D.; Guo, L.; Zhang, J.; Jones, L. R.; Chen, Z.; Pritchard, C.; Roeske, R. W. *J. Pept. Res.* **2001**, *57*, 301–306; (e) Ranganathan, D.; Samant, M. P.; Nagaraj, R.; Bikshapathy, E. *Tetrahedron Lett.* **2002**, *43*, 5145–5147; (f) Karle, I.; Ranganathan, D. *J. Mol. Struct.* **2003**, *647*, 85–96.
4. (a) Mlinarić-Majerski, K.; Pavlović, D.; Luić, M.; Kojić-Prodić, B. *Chem. Ber.* **1994**, *127*, 1327–1329; (b) Mlinarić-Majerski, K.; Pavlović, D.; Marinić, Ž *Tetrahedron Lett.* **1996**, *37*, 4829–4832; (c) Mlinarić-Majerski, K.; Pavlović, D.; Milinković, V.; Kojić-Prodić, B. *Eur. J. Org. Chem.* **1998**, 1231–1236; (d) Mlinarić-Majerski, K.; Veljković, J.; Kaselj, M.; Marchand, A. P. *Eur. J. Org. Chem.* **2004**, 2923–2927; (e) Šafar-Cvitaš, D.; Savin, B.; Mlinarić-Majerski, K. *Croat. Chem. Acta* **2004**, *77*, 619–625; (f) Mlinarić-Majerski, K.; Margeta, R.; Veljković, J. *Synlett* **2005**, 2089–2091.
5. (a) Mlinarić-Majerski, K.; Kragol, G. *Tetrahedron* **2001**, *57*, 449–457; (b) Mlinarić-Majerski, K.; Šumanovac Ramljak, T. *Tetrahedron* **2002**, *58*, 4893–4898; (c) Vujasinović, I.; Veljković, J.; Mlinarić-Majerski, K.; Molčanov, K.; Kojić-Prodić, B. *Tetrahedron* **2006**, *62*, 2868–2876; (d) For review, see: Mlinarić-Majerski, K. *Kem. Ind.* **2004**, *53*, 359–366.
6. (a) Horvat, Š.; Mlinarić-Majerski, K.; Glavaš-Obrovac, Lj.; Jakas, A.; Veljković, J.; Marczi, S.; Kragol, G.; Roščić, M.; Matković, M.; Milostić-Srb, A. *J. Med. Chem.* **2006**, *49*, 3136–3142; (b) Molčanov, K.; Kojić-Prodić, B.; Basarić, N.; Mlinarić-Majerski, K. *Acta Crystallogr.* **2006**, *E62*, o5406–o5408.
7. (a) Matković, M.; Veljković, J.; Mlinarić-Majerski, K.; Molčanov, K.; Kojić-Prodić, B. *J. Mol. Struct.* **2007**, *832*, 191–198; (b) Molčanov, K.; Kojić-Prodić, B.; Matković, M.; Mlinarić-Majerski, K. *Acta Crystallogr.* **2006**, *E62*, o4824–o4826.
8. Coe, S.; Kane, J. J.; Nguyen, T. L.; Toledo, L. M.; Wininger, E.; Fowler, F. W.; Lauher, J. W. *J. Am. Chem. Soc.* **1997**, *119*, 86–93.
9. (a) Makarević, J.; Jokić, M.; Perić, B.; Tomišić, V.; Kojić-Prodić, B.; Žinić, M. *Chem.—Eur. J.* **2001**, *7*, 3328–3341; (b) Makarević, J.; Jokić, M.; Raza, Z.; Štefanić, Z.; Kojić-Prodić, B.; Žinić, M. *Chem.—Eur. J.* **2003**, *9*, 5567–5580.
10. (a) Clariana, J.; García-Granda, S.; Gotor, V.; Gutiérrez-Fernández, A.; Luna, A.; Moreno-Mañas, M.; Vallribera, A. *Tetrahedron: Asymmetry* **2000**, *11*, 4549–4557; (b) Novikov, S. S.; Hardin, A. P.; Butenko, L. N.; Kulev, I. A.; Novakov, I. A.; Radèenko, S. S.; Burdenko, S. S. *Zh. Org. Khim.* **1980**, *16*, 1433–1435; (c) Geigy, J. R. Neth. Appl. 6,600,715, July 21, 1966. *Chem. Abstr.* **1996**, *65*, 16975.
11. Etter, M. C.; MacDonald, J. C.; Bernstein, J. *Acta Crystallogr.* **1990**, *B46*, 256–262.
12. Bernstein, J.; Davis, R. E.; Shimoni, L.; Chang, N.-L. *Angew. Chem., Int. Ed. Engl.* **1995**, *34*, 1555–1573.
13. Štefanić, Z. Ph.D. Thesis, University of Zagreb: Zagreb, Croatia, 2004.
14. Allen, F. H. *Acta Crystallogr.* **2002**, *B58*, 380–388.
15. Shkol'nikova, L. M.; Gasparyan, A. V.; Poznyak, A. L.; Bel'skii, V. K.; Dyatlova, N. M. *Koord. Khim.* **1990**, *16*, 50.
16. Allen, F. H.; Raithby, P. R.; Shields, G. P.; Taylor, R. *Chem. Commun.* **1998**, 1043–1044.
17. Allen, F. H.; Motherwell, W. D. S.; Raithby, P. R.; Shields, G. P.; Taylor, R. *New J. Chem.* **1999**, 25–34.
18. Harms, K.; Wocadlo, S. *XCAD-4, Program for Processing CAD4 Diffractometer Data*; University of Marburg: Germany, 1995.
19. North, A. C. T.; Philips, D. C.; Mathews, F. S. *Acta Crystallogr., Sect. A* **1968**, *24*, 351.
20. Farrugia, L. J. *J. Appl. Crystallogr.* **1999**, *32*, 837–838.
21. Sheldrick, G. M. *SHELXL97: Program for the Refinement of Crystal Structures*; Universität Göttingen: Germany, 1997.
22. Spek, A. L. *PLATON98: A Multipurpose Crystallographic Tool, 120398 Version*; University of Utrecht: Utrecht, The Netherlands, 1998.
23. Farrugia, L. J. *J. Appl. Crystallogr.* **1997**, *30*, 568.
24. Bruno, I. J.; Cole, J. C.; Edgington, P. R.; Kessler, M. K.; Macrae, C. F.; McCabe, P.; Pearson, J.; Taylor, R. *Acta Crystallogr.* **2002**, *B58*, 389–397.